

# Phase equilibria in the system ZnO–B<sub>2</sub>O<sub>3</sub>–SiO<sub>2</sub> at 950° C

M. A. EIDEM\*, B. R. ORTON, A. WHITAKER

*Department of Physics, Brunel University, Uxbridge, Middlesex UB8 3PH, UK*

Phase equilibria in the system ZnO–B<sub>2</sub>O<sub>3</sub>–SiO<sub>2</sub> were investigated at 950° C using quenching and X-ray powder diffraction techniques. The binary phases reported previously were confirmed but no ternary phases were found. Solid-solution effects were investigated for the primary and binary phases by comparison of patterns; no solid solutions were detected. There is a large liquid area in the high-B<sub>2</sub>O<sub>3</sub> corner of the phase diagram. It is found that zinc orthosilicate,  $\alpha$ -2ZnO · SiO<sub>2</sub>, dissolves in this to form a zinc-oxide-rich borosilicate liquid but 4ZnO · 3B<sub>2</sub>O<sub>3</sub> does not. There is also a liquid eutectic at approximate composition 65ZnO–25B<sub>2</sub>O<sub>3</sub>–10SiO<sub>2</sub> (wt%). The rate of volatilization and loss of B<sub>2</sub>O<sub>3</sub> was also investigated for 4ZnO · 3B<sub>2</sub>O<sub>3</sub> and it was concluded that although volatilization occurs, the loss was insufficient at the firing times and temperature used to invalidate the major features of the diagram.

## 1. Introduction

Compounds within both the ZnO–SiO<sub>2</sub> and ZnO–B<sub>2</sub>O<sub>3</sub> binary systems are known to exhibit fluorescent properties. In the ZnO–SiO<sub>2</sub> system, the mineral, willemite (zinc orthosilicate, 2ZnO · SiO<sub>2</sub>), gives a green fluorescence under ultraviolet radiation [1]. In addition, zinc orthosilicate may be activated by manganese to give a red-fluorescing form ( $\gamma$ -2ZnO · SiO<sub>2</sub>), a yellow-fluorescing form ( $\beta$ -2ZnO · SiO<sub>2</sub>) and a green-fluorescing form ( $\alpha$ -2ZnO · SiO<sub>2</sub>, willemite) [1]; although it appears that both the  $\gamma$  and  $\beta$  forms may be changed to the  $\alpha$  form, there is no record of the  $\alpha$  form changing to either of the others [1].

During their study of the ZnO–B<sub>2</sub>O<sub>3</sub> system, Harrison and Hummel [2] discovered that both the binary intermediates they found will fluoresce if activated with suitable amounts of manganese.

In spite of interest due to this fluorescence in both the binary systems there has been no attempt to determine the subsolidus phase equilibria of the ternary system, although some work has been reported on the ZnO<sub>2</sub>–B<sub>2</sub>O<sub>3</sub>–SiO<sub>2</sub> glasses [1, 3].

### 1.1. Previous work

As already mentioned, the ternary system has not been investigated in the subsolidus region but some work has been reported on ZnO–B<sub>2</sub>O<sub>3</sub>–SiO<sub>2</sub> glasses [1, 3]. In one case [1] the liquidus phases are given and this shows that this phase diagram is dominated (about two-thirds of the diagram) by a field of two immiscible liquids. In the second case the paper is really concerned with nuclear radioactive waste disposal using Na<sub>2</sub>O–ZnO–B<sub>2</sub>O<sub>3</sub>–SiO<sub>2</sub> glasses and the actual information on ZnO<sub>2</sub>–B<sub>2</sub>O<sub>3</sub>–SiO<sub>2</sub> glasses is rather sparse. However, data exist for all three binary systems.

A considerable amount of work has been completed on the ZnO<sub>2</sub>–B<sub>2</sub>O<sub>3</sub> phase diagram [1, 2, 4–14], much of it confusing and contradictory. This was summarized [15] in an article in which further results were reported. This report concluded that in the range 640 to 900° C, three zinc borates may be found;  $\alpha$ -3ZnO · B<sub>2</sub>O<sub>3</sub>, 4ZnO · 3B<sub>2</sub>O<sub>3</sub> and ZnO · 2B<sub>2</sub>O<sub>3</sub>. Up to 700° C only  $\alpha$ -3ZnO · B<sub>2</sub>O<sub>3</sub> and ZnO · 2B<sub>2</sub>O<sub>3</sub> are detected, while at 710° C 4ZnO · 3B<sub>2</sub>O<sub>3</sub> is obtained accompanied by the decomposition of ZnO · 2B<sub>2</sub>O<sub>3</sub>. However, the decomposition is very sluggish and all three compounds may coexist up to 900° C. According to one reference [2], 3ZnO<sub>2</sub> · B<sub>2</sub>O<sub>3</sub> is dimorphic with a transition temperature of 964° C, the high-temperature form being called  $\beta$  (this reference actually places this phase at a composition of 5ZnO · 2B<sub>2</sub>O<sub>3</sub>, as does some of the others). Since the summarizing article [15], the crystal structure of ZnO · 2B<sub>2</sub>O<sub>3</sub> has been determined [16]; those of 3ZnO · B<sub>2</sub>O<sub>3</sub> [14] and 4ZnO · 3B<sub>2</sub>O<sub>3</sub> [8–10] had already been reported and so the doubts on the compositions of the phases must be considered settled.

The ZnO–SiO<sub>2</sub> phase system at temperatures above 1300° C was originally studied by Bunting [17] who concluded that the only stable binary phase was zinc orthosilicate (2ZnO · SiO<sub>2</sub>). However, Schleede and Gruhl [18] examined melts of manganese-activated zinc orthosilicate and found that, depending upon the rate of cooling, one could obtain either green fluorescence (slow cooling), a yellow-fluorescent form (faster cooling) or a red-fluorescent form (chilled). These forms were subsequently named  $\alpha$ ,  $\beta$  and  $\gamma$  forms respectively [19]; the  $\alpha$  form corresponds to the mineral willemite. Ingerson, *et al.* [1] grew needle crystals of the  $\beta$  and  $\gamma$  forms and were able to determine the optical properties. In addition, they studied the

\*Present address: Marconi Defence Systems Ltd, Warren Lane, Stanmore, Middlesex.

thermal transitions and concluded that at temperatures in excess of 900°C, the  $\gamma$  form changes to the  $\beta$  form and then to the  $\alpha$  form. Williamson and Glasser [20] redetermined the phase diagram at temperatures above 1300°C; essentially their work confirms that of Bunting [17], but they also showed that  $\beta$  and  $\gamma$  forms could be obtained without the addition of manganese, but only from divitrified glasses; they could not be prepared from crystalline starting materials heated at subsolidus temperatures. They also showed that  $\alpha$ -zinc orthosilicate was the only stable binary compound at temperatures between 800°C and the liquidus.

Although other zinc orthosilicate polymorphs have been found at high pressures [21, 22] as well as one of zinc metasilicate,  $\text{ZnO} \cdot \text{SiO}_2$  [22], none of these have been found at atmospheric pressure.

The phase diagram for  $\text{B}_2\text{O}_3$ – $\text{SiO}_2$  has been studied many times, often with confusing and conflicting results. The most thorough work [23] (which also reviews the earlier results) concludes that there is no binary phase in this system under equilibrium conditions. This has been confirmed [24, 25].

## 2. Experimental procedure

### 2.1. Choice of firing temperature

The choice of the subsolidus firing temperature was governed by several conflicting factors:

(i) The necessity of ensuring complete solid-state reaction in the  $\text{ZnO}$ – $\text{SiO}_2$  system. The lowest solidus temperature in the phase diagram is 1432°C [17] or 1421°C [20], while the melting point of willemite is variously given as 1512°C [1, 17] or 1498°C [20].

(ii) The melting points of the various zinc borates. These have been determined by Harrison and Hummel [2] but attributed to slightly incorrect compositions. According to them,  $\text{ZnO} \cdot \text{B}_2\text{O}_3$  (really  $4\text{ZnO} \cdot 3\text{B}_2\text{O}_3$ ) melts at  $982 \pm 2^\circ\text{C}$  while  $\alpha$ - $5\text{ZnO} \cdot 2\text{B}_2\text{O}_3$  (really  $\alpha$ - $3\text{ZnO} \cdot \text{B}_2\text{O}_3$ ) transforms to  $\beta$ - $5\text{ZnO} \cdot 2\text{B}_2\text{O}_3$  at  $964 \pm 4^\circ\text{C}$  and melts at 1045°C.

(iii) The volatilization of  $\text{B}_2\text{O}_3$ . The melting point is given as 450°C [25] or in the range 455 to 475°C [26]. Studies of  $\text{B}_2\text{O}_3$  volatilization at 730°C have been carried out [23] and indicate that the weight loss of a pure  $\text{B}_2\text{O}_3$  sample is 7% after 1000 h. The rate of weight loss would appear to be linear. The first factor would ideally suggest a temperature of 1400°C or so, the second about 950°C and the third even lower.

As a result, compacts were made in the manner given below (Section 2.2). These corresponded to a composition of  $2\text{ZnO} \cdot \text{SiO}_2$  to which 3 wt % LiF was added as a mineralizer. Attempts were made to make  $\alpha$ - $2\text{ZnO} \cdot \text{SiO}_2$  at 900°C; examination of X-ray patterns from compacts fired at times ranging from 21.0 to 100.0 h indicated that in all cases the major phase was  $\text{ZnO}$ , while  $\alpha$ - $2\text{ZnO} \cdot \text{SiO}_2$  was a minor phase. What is more, the proportion of these phases (assessed from relative diffraction line strengths) was the same. In these circumstances it would appear that 900°C is too low for producing  $\alpha$ - $2\text{ZnO} \cdot \text{SiO}_2$  under equilibrium conditions.

At 950°C,  $\alpha$ - $2\text{ZnO} \cdot \text{SiO}_2$  could be made after firing for 89.3 h without need of a mineralizer, and so 950°C

was chosen as the firing temperature and no mineralizer was used in later work.

### 2.2. Thermal equilibrium diagram

The investigation commenced with examination of the starting materials and by preparing the binary compounds.

The starting materials were Analar zinc oxide (not less than 99.7% pure), Analar boric acid (not less than 99.5% pure) and silica (BDH (Pool, UK), precipitated approximately 98% pure, the remainder being mainly loss at 1000°C). For those few compacts where a mineralizer was added (see Section 2.1) Analar lithium fluoride (not less than 98% pure) was added. Quantities of zinc oxide, silica and lithium fluoride were stored inside the furnace at the firing temperature, until required for compact preparation.

For compact preparation, the appropriate quantities were mixed, ground to a fine powder under acetone, and pressed for 5 min in a 0.5 in. (13 mm) diameter steel die at 6000 lb in<sup>-2</sup> (41 MPa). No binder was used. All compacts were pre-fired at 400°C, removed, reground and repressed for the final firing.

Both pre-firing and firing were carried out in air with the compacts in open platinum boats. The temperature of firing was controlled at 950°C and the specimens air-quenched. Various firing times were used and these are mentioned in Table I.

After firing, a little of the compact was ground and used as an X-ray powder specimen which was examined in an 11.46 cm diameter Debye–Scherrer camera using filtered copper radiation.

## 3. Results

### 3.1. Zinc oxide–boric oxide binary system

Only two zinc borates were found in the system:  $4\text{ZnO} \cdot 3\text{B}_2\text{O}_3$  and  $\alpha$ - $3\text{ZnO} \cdot \text{B}_2\text{O}_3$ . The patterns agree with those reported previously [11, 13].  $\text{ZnO} \cdot 2\text{B}_2\text{O}_3$ , which had been found to coexist with  $4\text{ZnO} \cdot 3\text{B}_2\text{O}_3$  at temperatures up to 900°C [15], was not found at 950°C. It has already been mentioned that this zinc borate starts to decompose at a temperature of 710°C, but the decomposition was sluggish [15] and hence it could still be present at 900°C.

### 3.2. Zinc oxide–silicon dioxide binary system

It was confirmed that the only phase found in this system was  $\alpha$ - $2\text{ZnO} \cdot \text{SiO}_2$ , the mineral willemite.

### 3.3. Boric oxide–silicon dioxide binary system

It was confirmed that no binary was found in this system.

### 3.4. Thermal equilibrium diagram

During the course of the investigation into the thermal equilibrium diagram six binary and twenty-six ternary compacts were made and analysed. Table I lists these compacts, composition firing times, the interpretation of the X-ray diffraction patterns and the result of a visual inspection of the fired compacts. In some cases the presence of amorphous material was detected by X-rays, either by the lack of any crystalline phase or

TABLE I Specimens prepared, chemical analysis, firing times and X-ray analysis

| Compound or specimen No.              | Chemical composition (wt %) |                               |                  | Firing time (h) | Phase analysis                                 |  |  | Visual inspection |
|---------------------------------------|-----------------------------|-------------------------------|------------------|-----------------|--|--|--|-------------------|
|                                       | ZnO                         | B <sub>2</sub> O <sub>3</sub> | SiO <sub>2</sub> |                 | Major  | Minor  | Trace  |                   |
|                                       |                             |                               |                  |                 |  |  |  |                   |
| ZnO                                   | 100                         |                               |                  | 24.0            | ZnO  |  |  |                   |
| SiO <sub>2</sub>                      |                             |                               | 100              | 24.0            | $\alpha$ -cristobalite                         | Tridymite                                      |  |                   |
| 3ZnO · B <sub>2</sub> O <sub>3</sub>  | 77.8                        | 22.2                          |                  | 16.5            | $\alpha$ -3ZnO · B <sub>2</sub> O <sub>3</sub> |  |  |                   |
| 4ZnO · 3B <sub>2</sub> O <sub>3</sub> | 60.9                        | 39.1                          |                  | 5.9             | 4ZnO · 3B <sub>2</sub> O <sub>3</sub>          | $\alpha$ -3ZnO · B <sub>2</sub> O <sub>3</sub> |  |                   |
| ZnO · 2B <sub>2</sub> O <sub>3</sub>  | 36.9                        | 63.1                          |                  | 89.7            | 4ZnO · 3B <sub>2</sub> O <sub>3</sub>          |  |  |                   |
| 2ZnO · SiO <sub>2</sub>               | 73.0                        |                               | 27.0             | 89.2            | $\alpha$ -2ZnO · SiO <sub>2</sub>              |  | ZnO  |                   |
| 1                                     |                             | 63.5                          | 36.5             | 45.2            | Amorphous                                      |  |  | Glassy            |
| 2                                     |                             | 10.0                          | 90.0             | 45.7            | Amorphous                                      |  | Tridymite                                      | Glazed            |
| 3                                     | 10.0                        | 20.0                          | 70.0             | 41.5            | Amorphous                                      | $\alpha$ -2ZnO · SiO <sub>2</sub>              |  | Glassy            |
| 4                                     | 15.0                        | 10.0                          | 75.0             | 41.9            | Tridymite                                      |  |  | Glazed            |
|                                       |                             |                               |                  |                 | $\alpha$ -2ZnO · SiO <sub>2</sub>              |  |  |                   |
| 5                                     | 15.0                        | 70.0                          | 15.0             | 21.5            | Amorphous                                      |  |  | Glassy            |
| 6                                     | 20.0                        | 35.0                          | 45.0             | 22.5            | Amorphous                                      | $\alpha$ -2ZnO · SiO <sub>2</sub>              |  | Glassy            |
| 7                                     | 35.0                        | 22.0                          | 43.0             | 22.5            | $\alpha$ -2ZnO · SiO <sub>2</sub>              |  |  | Glassy            |
| 8                                     | 40.0                        | 11.0                          | 49.0             | 30.7            | $\alpha$ -2ZnO · SiO <sub>2</sub>              |  |  | Glazed            |
| 9                                     | 45.0                        | 5.0                           | 50.0             | 41.8            | $\alpha$ -2ZnO · SiO <sub>2</sub>              | Tridymite                                      |  | Neither           |
| 10                                    | 45.0                        | 20.0                          | 35.0             | 22.5            | $\alpha$ -2ZnO · SiO <sub>2</sub>              |  |  | Glazed            |
| 11                                    | 60.0                        | 7.0                           | 33.0             | 41.8            | $\alpha$ -2ZnO · SiO <sub>2</sub>              |  |  | Neither           |
| 12                                    | 30.0                        | 59.0                          | 11.0             | 21.6            | Amorphous                                      |  | 4ZnO · 3B <sub>2</sub> O <sub>3</sub>          | Glassy            |
| 13                                    | 49.6                        | 31.9                          | 18.5             | 41.5            | $\alpha$ -2ZnO · SiO <sub>2</sub>              |  |  | Glassy            |
| 14                                    | 60.7                        | 17.0                          | 22.3             | 41.5            | $\alpha$ -2ZnO · SiO <sub>2</sub>              |  |  | Glazed            |
| 15                                    | 25.0                        | 70.0                          | 5.0              | 20.4            | 4ZnO · 3B <sub>2</sub> O <sub>3</sub>          |  |  | Neither           |
| 16                                    | 45.0                        | 45.0                          | 10.0             | 21.5            | Amorphous                                      |  | 4ZnO · 3B <sub>2</sub> O <sub>3</sub>          | Glassy            |
| 17                                    | 55.0                        | 40.0                          | 5.0              | 24.4            | 4ZnO · 3B <sub>2</sub> O <sub>3</sub>          | $\alpha$ -2ZnO · SiO <sub>2</sub>              |  | Neither           |
| 18                                    | 58.0                        | 30.0                          | 12.0             | 20.5            | 4ZnO · 3B <sub>2</sub> O <sub>3</sub>          | $\alpha$ -2ZnO · SiO <sub>2</sub>              |  | Glassy            |
| 19                                    | 65.0                        | 15.0                          | 20.0             | 24.4            | $\alpha$ -2ZnO · SiO <sub>2</sub>              | 4ZnO · 3B <sub>2</sub> O <sub>3</sub>          |  | Neither           |
| 20                                    | 63.0                        | 32.0                          | 5.0              | 1.5             | Amorphous                                      |  |  | Glassy            |
| 21                                    | 67.0                        | 19.0                          | 14.0             | 41.5            | $\alpha$ -2ZnO · SiO <sub>2</sub>              |  |  | Glazed            |
| 22                                    | 70.0                        | 10.0                          | 20.0             | 45.7            | $\alpha$ -2ZnO · SiO <sub>2</sub>              |  | $\alpha$ -3ZnO · B <sub>2</sub> O <sub>3</sub> |                   |
| 23                                    | 76.0                        | 15.0                          | 9.0              | 92.0            | $\alpha$ -3ZnO · B <sub>2</sub> O <sub>3</sub> |  |  |                   |
|                                       |                             |                               |                  |                 | $\alpha$ -2ZnO · B <sub>2</sub> O <sub>3</sub> |  |  |                   |
| 24                                    | 80.0                        | 5.0                           | 15.0             | 49.9            | $\alpha$ -2ZnO · SiO <sub>2</sub>              |  | $\alpha$ -3ZnO · B <sub>2</sub> O <sub>3</sub> |                   |
|                                       |                             |                               |                  |                 | ZnO  |  |  |                   |
| 25                                    | 82.0                        | 13.0                          | 5.0              | 28.0            | ZnO  | $\alpha$ -3ZnO · B <sub>2</sub> O <sub>3</sub> |  |                   |
|                                       |                             |                               |                  |                 |  | $\alpha$ -2ZnO · SiO <sub>2</sub>              |  |                   |
| 26                                    | 90.0                        | 5.0                           | 5.0              | 30.7            | ZnO  |  | $\alpha$ -2ZnO · SiO <sub>2</sub>              |                   |
|                                       |                             |                               |                  |                 |  |  | $\alpha$ -3ZnO · B <sub>2</sub> O <sub>3</sub> |                   |

by the high background recorded on the film; in others there was no evidence of this nature and the presence of amorphous material (glass) was obtained from a visual inspection alone. The compatibility triangles consistent with these results are given in Fig. 1.

X-ray patterns containing binary phases were compared. From this comparison there appeared to be no evidence of solid-solution effects in the binary phases; however, many patterns lacked sharp lines in the back-reflection region and because of this the existence of some solubility cannot be discounted.

#### 4. Discussion

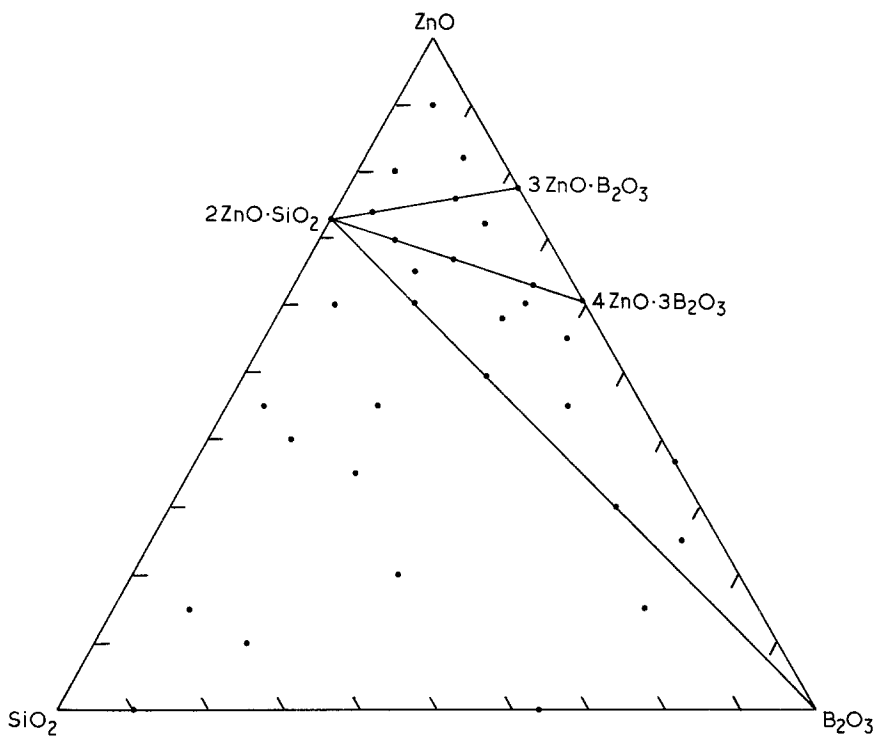
The lack of solid solution, mentioned in the previous section, is not unexpected. The published binary phase diagrams of zinc oxide–boric oxide [2], zinc oxide–silicon dioxide [17, 20] and boric oxide–silicon dioxide [23] suggest that there are no solid solutions in any of them. Van Vlack [26] points out that in close-packed crystal structures there can be extensive solid solution if the size of the host and substitutional ions do not differ by more than 15%, but that this limitation may be relaxed if the structures are not close-packed. In addition, solid solution is limited if the host and sub-

stitution atoms have different valency, or for compounds having different structures.

Based on the ionic radius of O<sup>2-</sup> as 0.140 nm for sixfold coordination, Shannon and Prewitt [27] give the ionic radii for sixfold coordination as Zn<sup>2+</sup> 0.075 nm, Si<sup>4+</sup> 0.040 nm and B<sup>3+</sup> 0.023 nm. In their oxides, zinc and silicon have fourfold coordination and boron threefold. The ionic radii corresponding to these coordination numbers are 0.060, 0.026 and 0.002 nm, respectively. Whichever figures are used, in either case the three ions have widely different radii. In addition, the three ions have different valencies. Thus it can be seen that the conditions are not favourable for the formation of solid solutions.

A major concern with firing at such a high temperature as 950°C was the inevitable loss of B<sub>2</sub>O<sub>3</sub> due to volatilization. It has already been shown that the weight loss of a pure B<sub>2</sub>O<sub>3</sub> sample is 7% after 1000 h at 730°C [23]. Thus the volatilization was studied at 950°C. Rather than use a pure B<sub>2</sub>O<sub>3</sub> sample (which is rather artificial in view of the compositions studied), the binary 4ZnO · 3B<sub>2</sub>O<sub>3</sub> was studied. This was chosen because of its relatively high B<sub>2</sub>O<sub>3</sub> content (39.1 wt %); there were only six compacts richer in B<sub>2</sub>O<sub>3</sub> that were

Figure 1 Phase equilibrium in the system  $\text{ZnO}-\text{B}_2\text{O}_3-\text{SiO}_2$  at  $950^\circ\text{C}$ .



studied. Also this compound produces a very distinctive X-ray pattern which would allow for easier X-ray interpretation if required. The results given in Fig. 2 show that there is an initial higher  $\text{B}_2\text{O}_3$  loss before the loss rate becomes linear and significantly smaller. This initial loss is no doubt due to volatilization from the surface. Even including this initial surface loss, the total loss corresponded to approximately 2% after 20 h and some 3.5% after 40 h. Thus, although the actual compositions must be somewhat different to the nominal values in Table I and Fig. 1, the difference is insufficient to invalidate the proposed phase diagram.

The proposed phase diagram suggests that silica exists in a considerable area of the sub-solidus phase diagram, yet tridymite was only detected in three

specimens (Nos 2, 4 and 9). Of course this is because of the low melting point of  $\text{B}_2\text{O}_3$ ,  $450^\circ\text{C}$  [28] or  $455$  to  $475^\circ\text{C}$  [29]; this means that the diagram determined is not subsolidus over a considerable area. In fact, according to the data on the  $\text{B}_2\text{O}_3-\text{SiO}_2$  binary diagram [23], this system is liquid at  $950^\circ\text{C}$  from  $\text{B}_2\text{O}_3$  to a composition of approximately  $33\text{B}_2\text{O}_3-67\text{SiO}_2$  (wt %). Assuming that this boundary is not affected by the presence of  $2\text{ZnO} \cdot \text{SiO}_2$ , this means that tridymite would only be present in five specimens (Nos 2, 3, 4, 8 and 9) and in two of these (Nos 3 and 8) the amount would be less than 13%.

It has already been reported [1], that at the liquidus most of the phase diagram is dominated by two immiscible liquids, one of which is almost pure

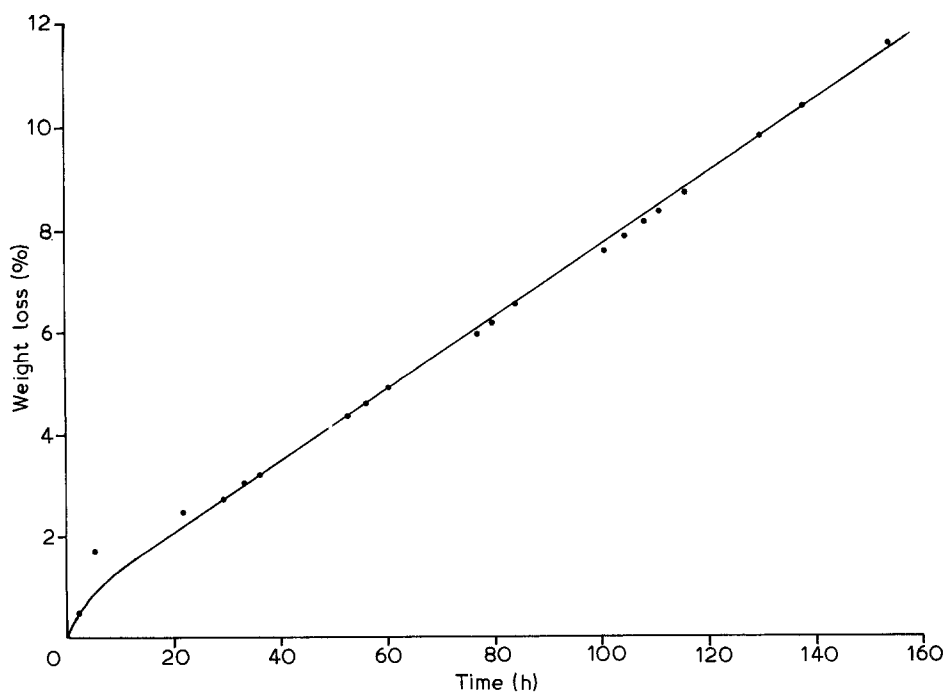


Figure 2 Volatilization of boric oxide from  $4\text{ZnO} \cdot 3\text{B}_2\text{O}_3$  at  $950^\circ\text{C}$ .

TABLE II Specimens of 63.0ZnO–32B<sub>2</sub>O<sub>3</sub>–5SiO<sub>2</sub> (wt %) fired at various temperatures

| Temperature (°C) | Firing time (h) | Phase analysis                        |                         |                                      |
|------------------|-----------------|---------------------------------------|-------------------------|--------------------------------------|
|                  |                 | Major                                 | Minor                   | Trace                                |
| 800              | 24.5            | 4ZnO · 3B <sub>2</sub> O <sub>3</sub> | 2ZnO · SiO <sub>2</sub> | 3ZnO · B <sub>2</sub> O <sub>3</sub> |
| 850              | 22.5            | 4ZnO · 3B <sub>2</sub> O <sub>3</sub> | 2ZnO · SiO <sub>2</sub> | 3ZnO · B <sub>2</sub> O <sub>3</sub> |
| 900              | 21.0            | 4ZnO · 3B <sub>2</sub> O <sub>3</sub> | 2ZnO · SiO <sub>2</sub> | 3ZnO · B <sub>2</sub> O <sub>3</sub> |
| 910              | 73.0            | 4ZnO · 3B <sub>2</sub> O <sub>3</sub> | 2ZnO · SiO <sub>2</sub> | 3ZnO · B <sub>2</sub> O <sub>3</sub> |
| 930              | 24.0            | 4ZnO · 3B <sub>2</sub> O <sub>3</sub> |                         | 2ZnO · SiO <sub>2</sub>              |
| 940              | 24.0            | Sample melted                         |                         |                                      |

B<sub>2</sub>O<sub>3</sub>–SiO<sub>2</sub> (probably containing less than 1% ZnO) and a zinc-oxide-rich borosilicate liquid, whose composition is believed to be near 60.7ZnO–19.1B<sub>2</sub>O<sub>3</sub>–20SiO<sub>2</sub> [1] (i.e. near Specimen No. 14). The presence of this two-liquid region has been subsequently confirmed [3]. In addition, it is pointed out by Taylor and Owen [3] that there is secondary segregation of SiO<sub>2</sub>-rich particles within the zinc-rich phase, but they only mention detailed work on one sodium-free composition (18ZnO–18B<sub>2</sub>O<sub>3</sub>–64SiO<sub>2</sub>) at 1300°C, and so it is not known how extensively this secondary segregation occurs, particularly as the only composition reported contains such a large proportion of SiO<sub>2</sub>.

This zinc-oxide-rich borosilicate liquid exists at 950°C but not with the same composition [1] as at the liquidus. Assuming the nominal compositions in Table I, a mineralogical analysis (i.e. a percentage phase analysis) suggests that Specimens 12 and 16 contain 40.7 and 37.0 wt % 2ZnO · SiO<sub>2</sub>, respectively, but in neither case is 2ZnO · SiO<sub>2</sub> detected, while it is detected in Specimens 3 and 4 in which the amounts of 2ZnO · SiO<sub>2</sub> are 14.7 and 20.5 wt %, respectively. This is no doubt due to the 2ZnO · SiO<sub>2</sub> dissolving in the excess B<sub>2</sub>O<sub>3</sub>; excess B<sub>2</sub>O<sub>3</sub> being defined as that remaining after allowing for the pure saturated borosilicate liquid mentioned earlier [1, 3], of approximate composition 33B<sub>2</sub>O<sub>3</sub>–67SiO<sub>2</sub> [23] at 950°C. The amounts of excess B<sub>2</sub>O<sub>3</sub> are 58.8 and 33.4 wt % in specimens 12 and 16, respectively, but zero in Specimens 3 and 4. In fact in the four specimens where 2ZnO · SiO<sub>2</sub> would be expected but not found (Nos. 5, 12, 15 and 16) there is a minimum of 33.4 wt % excess B<sub>2</sub>O<sub>3</sub>. However, with one exception, 4ZnO · 3B<sub>2</sub>O<sub>3</sub> was detected in all specimens where it would be expected. As the exception, Specimen 14 contained only 0.7 wt % 4ZnO · 3B<sub>2</sub>O<sub>3</sub>; this would be too small to detect using X-ray powder techniques, and so it appears that 2ZnO · SiO<sub>2</sub> will dissolve in free liquid B<sub>2</sub>O<sub>3</sub> while 4ZnO · 3B<sub>2</sub>O<sub>3</sub> will not.

This analysis is not meant to imply that a pure borosilicate glass of the saturated composition exists over all the B<sub>2</sub>O<sub>3</sub>-rich part of the diagram, but simply that the solution of 2ZnO · SiO<sub>2</sub> to form a zinc-oxide-rich borosilicate glass appears to depend upon the amount of excess B<sub>2</sub>O<sub>3</sub>.

In addition to the large liquid (glassy) area in the high-B<sub>2</sub>O<sub>3</sub> corner of the diagram, there is a small one in a region of Specimen 20 on the 2ZnO · SiO<sub>2</sub>–4ZnO · 3B<sub>2</sub>O<sub>3</sub> tie-line. This suggests a eutectic along this tie-

line, but to test that there was no intermediate ternary compound, a series of specimens all with the composition of Specimen 20 (63.0ZnO–32.0B<sub>2</sub>O<sub>3</sub>–5.0SiO<sub>2</sub>) were made, fired at temperatures between 800 and 940°C and X-ray analysed (Table II). This indicates that there is no ternary phase along this tie-line and there there is a eutectic between Specimens 20 and 21 (67ZnO–19B<sub>2</sub>O<sub>3</sub>–14SiO<sub>2</sub>).

## References

1. E. INGERSON, G. W. MOREY and O. F. TUTTLE, *Amer. J. Sci.* **246** (1948) 31.
2. D. E. HARRISON and F. A. HUMMEL, *J. Electrochem. Soc.* **103** (1956) 491.
3. P. TAYLOR and D. G. OWEN, *J. Amer. Ceram. Soc.* **64** (1981) 360.
4. N. A. TOROPOV and P. F. KONOVALOV, *Doklady Akad. Nauk. SSSR* **66** (1949) 1105.
5. H. E. SWANSON and E. TATGE, *J. Res. Nat. Bur. Stand.* **46** (1951) 318.
6. YU. S. LEONOV, *Doklady. Akad. Nauk. SSSR* **114** (1957) 976 (*Soviet Phys. "Doklady"* **2** (1957) 261).
7. *Idem*, *Zhur. Neorg. Khim.* **3** (1958) 1245.
8. P. SMITH, S. GARCIA-BLANCO and L. RIVOIR, *Anales Real Soc. Espan. Fis. Quim.* **57A** (1961) 263.
9. *Idem.*, *Z. Krist.* **115** (1961) 460.
10. *Idem*, *ibid.* **119** (1964) 375.
11. H. BAUER, *Z. Anorg. Chem.* **320** (1963) 306.
12. C. E. WEIR and R. A. SCHROEDER, *J. Res. Nat. Bur. Stand.* **68A** (1964) 465.
13. J. FAYOS, S. GARCIA-BLANCO and L. RIVOIR, *Anales. Real. Soc. Espan. Fis. Quim.* **62A** (1966) 297.
14. S. GARCIA-BLANCO and J. FAYOS, *Z. Krist.* **127** (1968) 145.
15. A. WHITAKER, *J. Mater. Sci.* **7** (1972) 189.
16. M. MARTINEZ-RIPOLL, S. MARTINEZ-CARRERA and S. GARCIA-BLANCO, *Acta. Crystallogr.* **B27** (1971) 672.
17. E. N. BUNTING, *Bur. Stand. J. res.* **4** (1940) 134; quoted in E. M. Levin, C. R. Robins and H. F. McMurdie, "Phase Diagrams for Ceramists" (American Ceramic Society, 1964) Fig. 302.
18. A. SCHLEEDE and A. GRUHL, *Z. Electrochem.* **29** (1923) 411.
19. H. W. LEVERENZ and F. SEITZ, *J. Appl. Phys.* **10** (1939) 479.
20. J. WILLIAMSON and F. P. GLASSER, *Phys. Chem. Glasses* **5** (1964) 52.
21. A. E. RINGWOOD and A. MAJOR, *Nature* **215** (1967) 1367.
22. YASUHIKO SYONO, SYUN-ITI AKIMOTO and YOSHITO MATSUI, *J. Solid State Chem.* **3** (1971) 369.
23. T. J. ROCKET and W. R. FOSTER, *J. Amer. Ceram. Soc.* **48** (1965) 75.
24. R. BAYLOR Jr and J. J. BROWN, Jr, *ibid.* **59** (1976) 21.
25. T. D. LONSDALE and A. WHITAKER, *J. Mater. Sci.* **13** (1978) 1503.
26. L. H. VAN VLACK, "Physical Ceramics for Engineers" (Addison-Wesley, Reading, Mass., 1964) p. 52.
27. R. D. SHANNON and C. T. PREWITT, *Acta Crystallogr.* **B25** (1969) 925.
28. F. C. KRACEK, G. W. MOREY and H. E. MERWIN, *Amer. J. Sci.* **35A** (1938) 143.
29. J. D. MACKENZIE and W. F. CLAUSSEN, *J. Amer. Ceram. Soc.* **44** (1961) 79.

Received 29 January  
and accepted 15 April 1987